Superconductors for magnets I

René Flükiger

CERN
TE-MSC

Outline: Low T_c Superconductors (LTS)

I Introduction, Definitions
II Physical properties of superconducting Materials:
NbTi and Nb_3Sn
III Thermal Stability criteria
IV The system NbTi, properties and fabrication
V The system Nb_3Sn
A. Superconducting properties of the A15 phase
B. Wire fabrication and critical current densities
C. Calorimetric analysis of Nb_3Sn wires

I. Introduction, definitions

Actual situation of superconductor wires

Round wires

NbTi Still the most used wires: ~ 90% (MRI, accelerators)

Nb_3Sn > 5% (NMR, lab magnets, accelerators as LHC Upgrade)

MgB_2 Low costs; Niche applications at 10 – 25 K (open MRI, LINK)

Bi-2212 Future accelerators at >20T. Problem: mechanical stability

Tapes

Bi,Pb(2223) Cables, motors at T< 30K. Problems: costs, < 1 T at 77K)

YBCO Cables, Current limiters, Wind generators,…….
(Main problems: costs, limited lengths)
Commercially available: < 500 m SuperPower, USA
< 500 m at Fujikura, Japan

Other high field superconductors

$Ba_{0.6}K_{0.4})Fe_2As_2$ Pnictides: promising for high field magnets (B_{c2} > 70T), but not yet at the industrial level. Problems: toxicity of As, complex metallurgy.

$PbMo_6S_8$ Chevrel phases. B_{c2}>50T!
Problems: Reaction at > 1000°C, very difficult deformation, no prestress.

Technically interesting superconductors

Compound	Year	T_c (K)	$B_{c2}(0)$ (T)	ξ (nm)	
NbTi	1960	9.5	14.6	~ 6	
Nb_3Sn	1953	18.3	24 - 28	~4	LTS
$PbMo_6S_8$	1970	15	60	2.2	
Nb_3Ge	1972	23	38	~4	
Nb_3Al	1975	19	33	~4	
MgB_2	2001	39	39^a_{bulk}; 60^a_{films}	5	
$Bi_2Sr_2Ca_1Cu_2O_8$	1989	94	> 100[a]	1 - 2	HTS
$Bi_2Sr_2Ca_2Cu_3O_{10}$	1989	110	> 100[a]	1 - 2	
$YBa_2Cu_3O_7$	1988	92	> 100[a]	1 - 2	
$(Ba_{0.6}K_{0.4})Fe_2As_2$	2007	38	70 - >135[a]	2 - 3	

Cooling Regime for various Superconducting wires

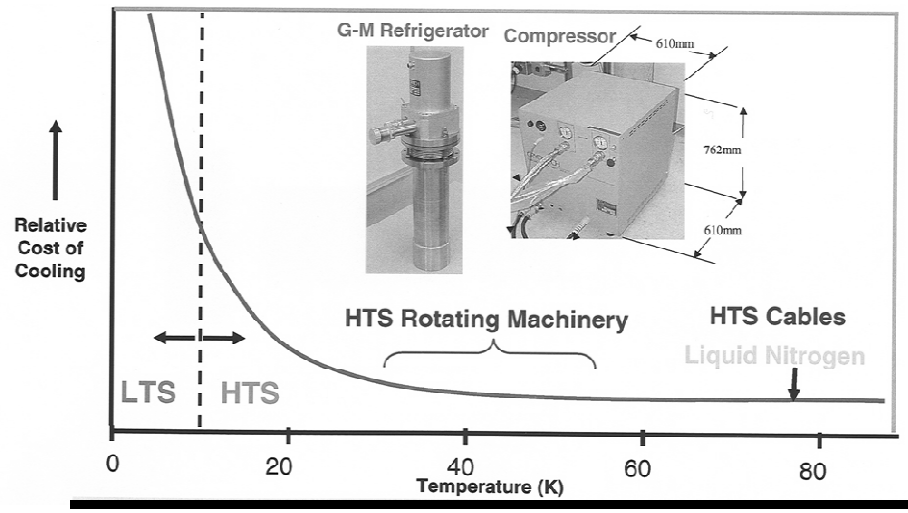

Applied Superconductivity: Definitions

Definitions

Supercond. transition temperature:	T_c [K]
Critical current:	I_c [A]
Critical current density:	j_c [A/cm^2]; j_c [A/mm^2]
Critical magnetic field:	B_{c2} [T]
Exponential *n* factor:	n: $U \sim I^n$

Critical surface in type II superconductors

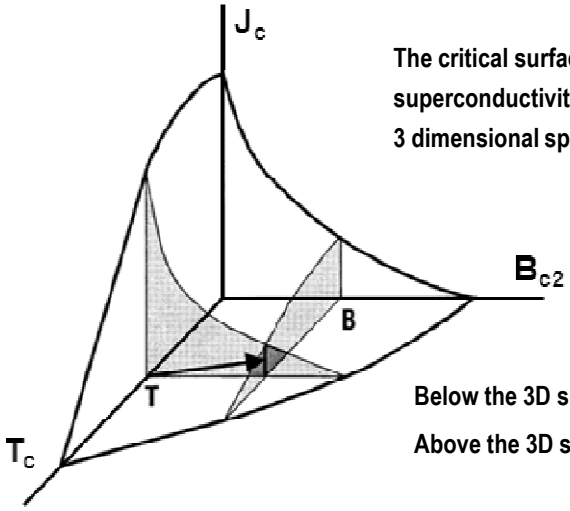

The critical surface is the boundary between superconductivity and normal resistivity in the 3 dimensional space.

Below the 3D surface: superconductivity.

Above the 3D surface: normal state, with $R \neq 0$.

Transport Measurement of J_c

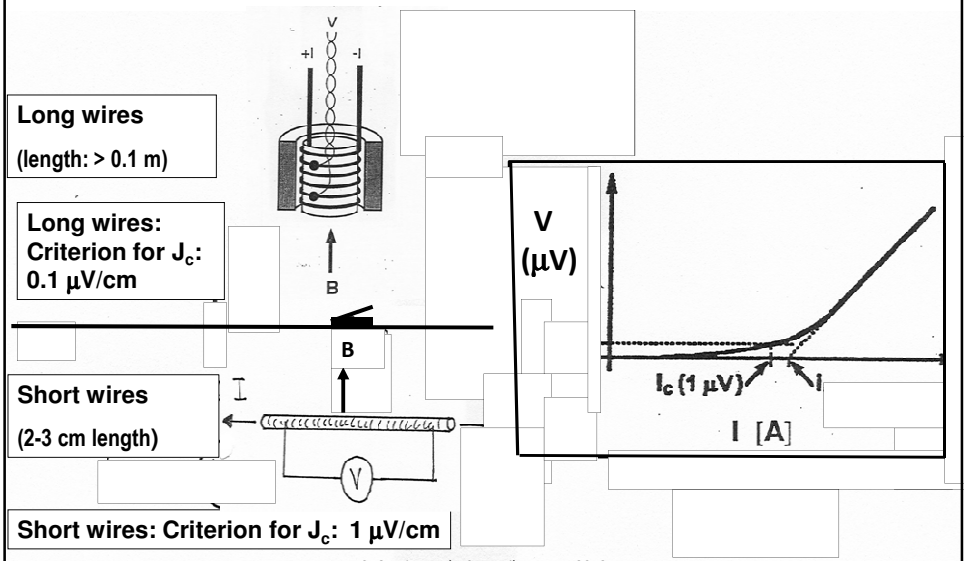

Long wires

(length: > 0.1 m)

Long wires: Criterion for J_c: 0.1 μV/cm

Short wires

(2-3 cm length)

Short wires: Criterion for J_c: 1 μV/cm

Measurement of Industrial Nb_3Sn wires

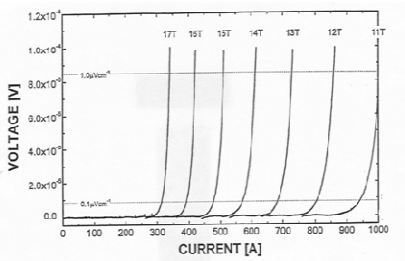

Resistive superconducting transition at various magnetic fields

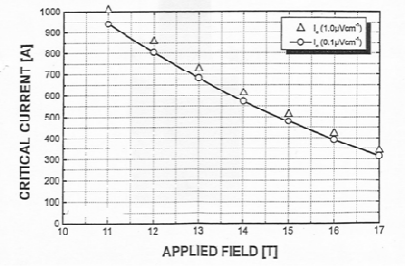

Variation of critical current vs. applied magnetic field B

The exponential *n* factor

The *n* factor is an empirical quantity describing the quality of the wire:

* surface state of the filaments
* homogeneity along the wire axis («sausaging»)

Definition: $V \sim I^n$ at a given operational B and T

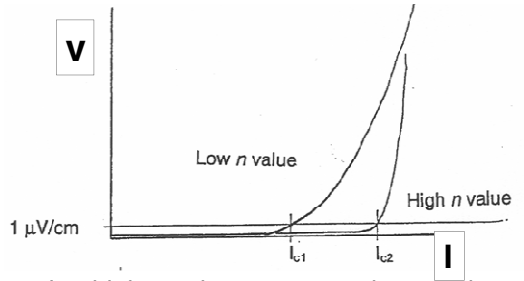

In general, a high *n* value corresponds to a wire of higher quality

Required: $n > 30$ at operational B and T.

Highest *n* values for NMR magnets

II. Physical properties of superconducting Materials: NbTi and Nb_3Sn

The upper critical magnetic field B_{c2}

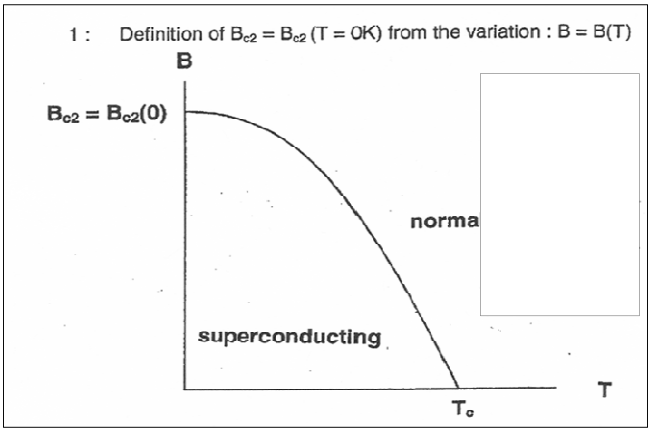

Upper critical fields of metallic (LTS) superconductors

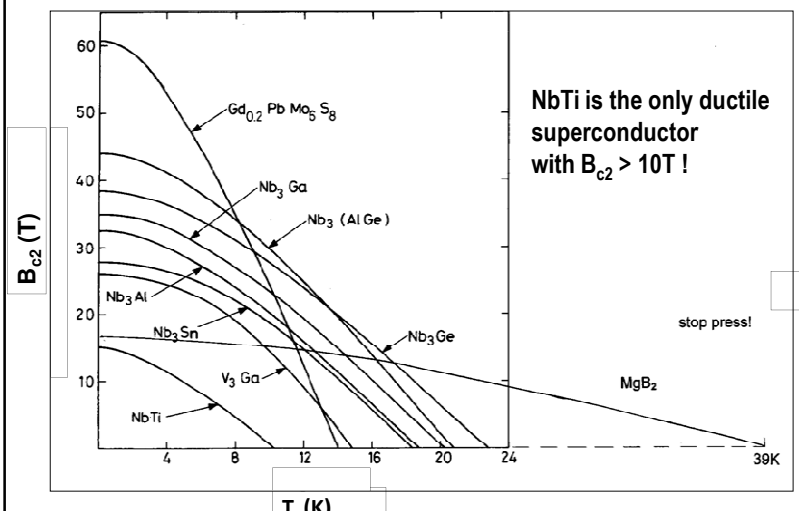

NbTi is the only ductile superconductor with B_{c2} > 10T !

Kramer extrapolation: estimation of B_{c2} at a given T

$B_{c2}(0)$ is determined by measuring $B_{c2}(T)$ either resistively or inductively.

In the case of wires, where I_c is known, one uses the Kramer extrapolation: the function $B^{¼}\, I_c^{1/2}$ (T) vs. B is extrapolated to B = 0 $\Rightarrow B_{c2}^*|_T$

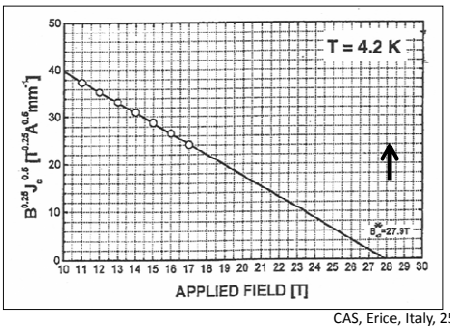

For magnets, one defines usually:

NbTi : B_{c2}^*(1.9 K),
Nb_3Sn: B_{c2}^*(4.2K).

These extrapolated values may differ from B_{c2}(4.2K) or B_{c2}(1.9K) determined by a direct measurement.

The Kramer extrapolation

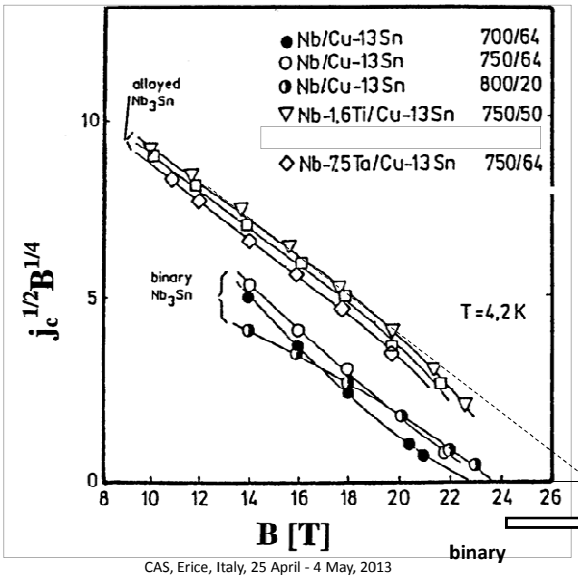

Flux pinning in superconducting wires

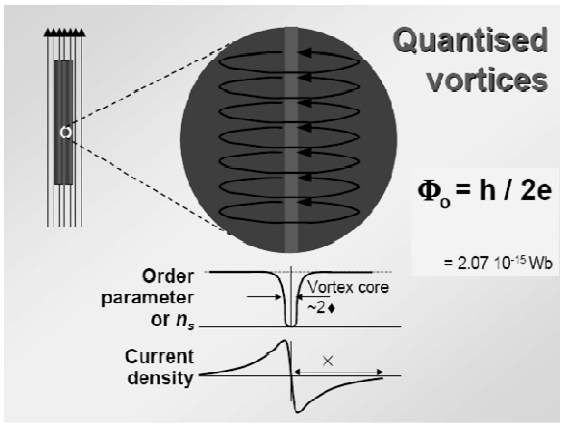

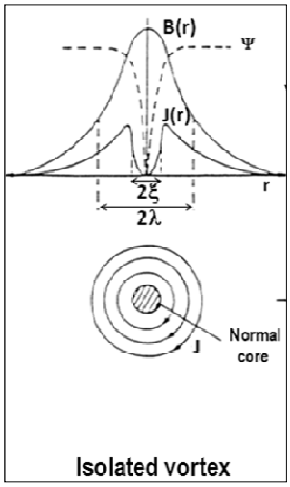

How to imagine a vortex?

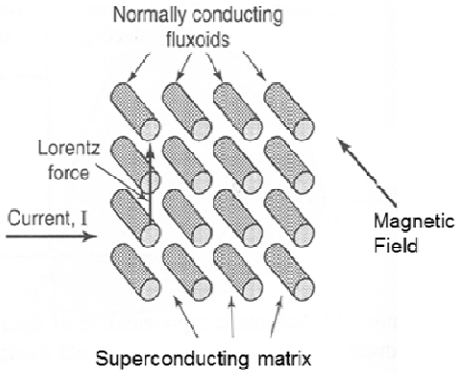

Tornado
* Speed zero at the center
* V_{max} outside of the tube *
Diameter: > 100 m

Vortex
* T_c = 0 inside (normal)
* $J_c \neq 0$ outside of the vortex
* « Diameter »: < 10 nm

Possible pinning mechanisms

J_c in a wire is zero, unless vortices can be «pinned» !

Microscopic defects provide pinning sites:

- Precipitates
- Dislocations
- Twin boundaries, stacking faults
- Irradiation tracks
- Grain boundaries

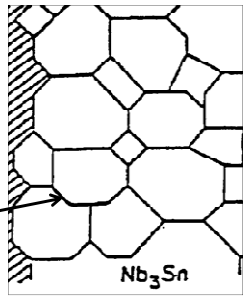

Grain boundaries: main contribution to pinning in LTS

Correlation between grain size and J_c in LTS

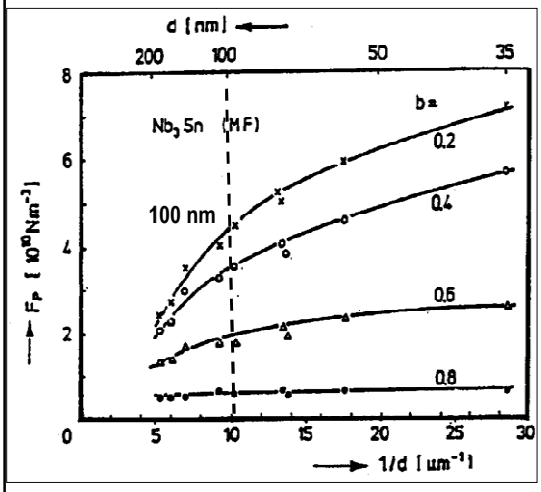

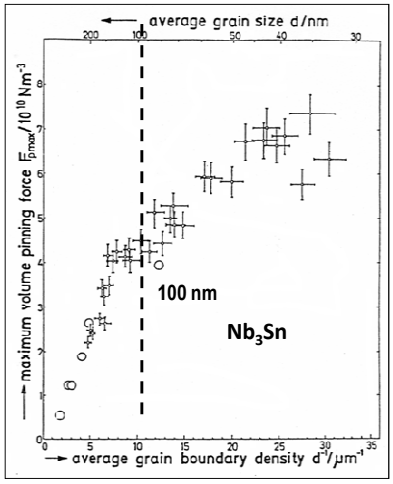

Schauer and Schelb, 1980

Nb_3Sn: effects of grain size and pinning force

Nb_3Sn bronze route wire

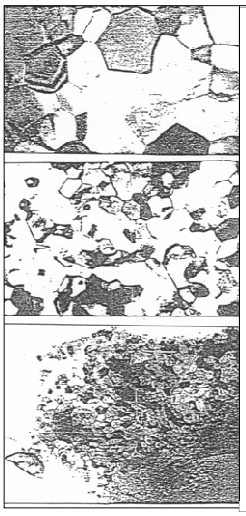

800 °C/48h
d_k =200 nm
$F_{pmax} = 2.5 \times 10^{10}$ Nm^{-3}

680 °C/48h
d_k = 85 nm
$F_{pmax} = 5.1 \times 10^{10}$ Nm^{-3}

600 °C/200h
d_k = 40 nm
$F_{pmax} = 6.8\ 10^{10}$ Nm^{-3}

Increase of grain size with reaction temperature

The Pinning Force

The motion of a flux line submitted to a magnetic field can be stopped by introducing pinning centers, thus leading to an energy reduction.

Maximum pinning force per flux tube :
$$\vec{f_p} = -(\vec{j_c} \times \vec{\Phi_o})$$
Maximum pinning force per volume :
$$\vec{F_p} = n\ \vec{f_p} = -(\vec{j_c} \times \vec{B})$$

In a type II superconductor in the mixed state, j_c is limited by the motion of flux lines.
Lorentz force on each flux line : $\vec{F_L} = \vec{j} \times \vec{\Phi_o}$

Flux motion leads to energy dissipation, thus to local heating.

Energy dissipation : $P = j\ E = \vec{j}(\vec{v} \times \vec{B})$

There is energy dissipation when $F_P > F_L$, i.e. when the Lorentz force is larger than the pinning force.

Variation of the Lorentz force F_p with reduced field

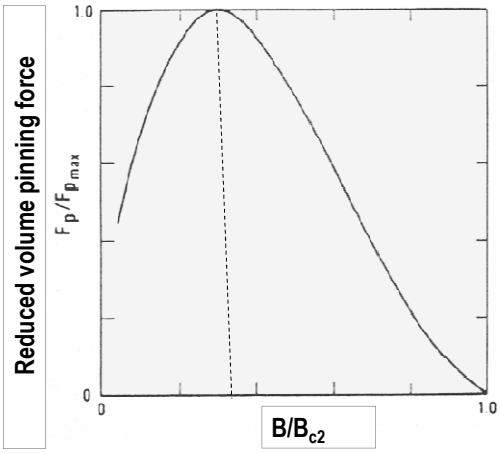

Reduced field: $b = B/B_{c2}$

$F(b) \sim b^p(1-b)^q$

III. Thermal Stability of a wire submitted to a current

Local and/or temporary perturbations may lead to thermal instability and to a quench.

Consider a wire with T_c submitted to I in bath T_b. Stable operation conditions: $T_c > T_b$

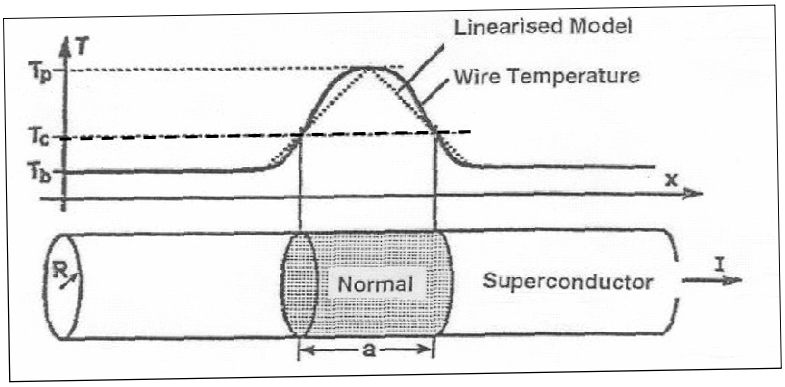

Why multifilamentary superconducting wires?

Suppose a local perturbation causing : $T = T_p > T_c$

$\Longrightarrow$ * a resistive zone develops in the wire
* Joule heat is built up locally.

Energy to be evacuated to restore the superconducting state comprises:
*the energy leading to the perturbation, and
*the energy produced by the Joule heat.

Three different power terms have to considered:

1: The Joule heat

$$P_{joule} = R_n I^2 = \rho_n a j^2 \pi R^2$$

where $j = I / \pi R^2$, and r_n = normal resistivity.

2. Heat conduction through the wire

Heat from the resistive zone to the neighbouring superconducting region:

$P_{conduction} = 2\pi R^2 \lambda \, dT/dx = 2\pi R^2 \lambda \, dT'$,
where λ = thermal conductivity
T' = temp. gradient in perturbed zone
= $dT/dx = 2 (T_p - T_c)/a$

3. Heat transfer to the bath, in a slice of thickness x

$dP_{bath} = 2\pi R h [T(x) - T_b] dx$, and
$P_{bath} = 2\pi R a h [(T_c - T_b) + a T']$,
where h = heat transfer coefficient (to the bath)

The thermal stability limit is now given by :

$$P_{joule} < P_{conduction} + P_{bath}$$

$$\Longrightarrow \quad \rho_n I^2 < 2\lambda \, dT' \, 1/a + hT'/2R \, a + 2h/R(T_c - T_b) \equiv f(a)$$

Regions of instability in a wire

$$\rho_n I^2 < 2\lambda\, dT'\, 1/a + hT'/2R\, a + 2h/R(T_c - T_b) \equiv f(a)$$

Graphical representation showing the regions of instability

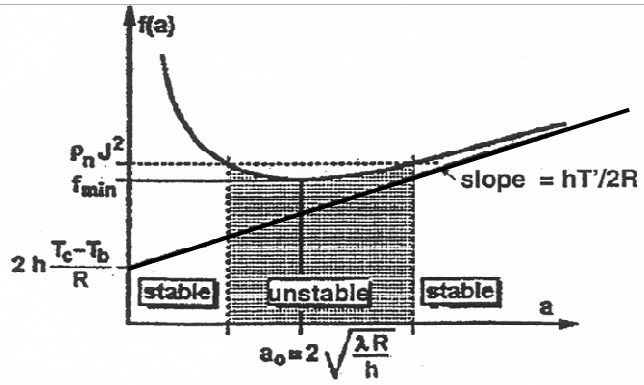

Stability criteria for wires

In order to satisfy the stability critierion, following parameters have to be optimized, leading to the actual multifilamentary wire configuration :

a : Temperature : The difference $(T_c - T_b)$ must be as large as possible → High T_c is important

b : Wire radius R: R should be as small as possible
→ small filament diameters, multifilamentary configuration in industrial wires

c: Heat conductivity λ: λ must be as high as possible
→ each filament in an industrial wire is surrounded by with a highly conducting Cu matrix

d: Heat transfer h: h must be minimized
→ The Cu matrix is also effective in providing a better heat transfer to the bath.

Criteria for stability and applicability of superconducting wires

1 : Chemical stability
2 : Mechanical stability :
Bulk superconductors (except NbTi) break at **ε <0.05 % !**
→ microcomposite (multifilamentary) configuration
Filament size: < 5 - 30 μm
Wires: Irreversible strain: $\varepsilon_{irr} > 0.4$ %
3 : Cryogenic stability : presence of Cu as stabilizer
High thermal conductivity of Cu
→ a minimum quantity of stabilizer is required (> 23% Cu)
4 : Electromagnetic stability :
Low AC coupling losses required → Twisting of wires
5 : Low material costs
6: Length: > 1 km

Typical wire configuration: 1'000 -10'000 filaments
5 - 30 mm filament size
25 cm twist pitch

Intergrain boundary at the high Sn limit of Bronze Route Wires

LTS:
Defects at grain boundaries: breakage of periodicity creates normalconducting regions: Vortices, will pin the flux lines

Grain boundaries are the main factor for the enhancement of Jc in superconducting wires

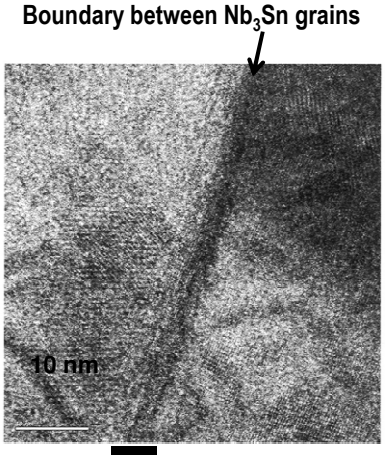

R. Flükiger and M. Cantoni, 2005

4 nm: ~ Coherence length ξ_0

IV. The system NbTi

Crystal structure and phase diagram

NbTi: T_c = 10 K, B_{c2} = 14 T

Body cubic cented structure

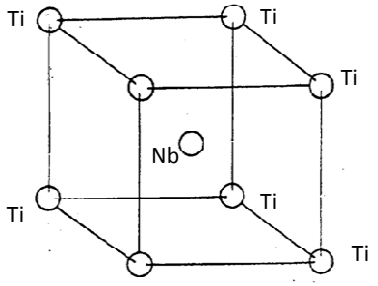

Phase diagram

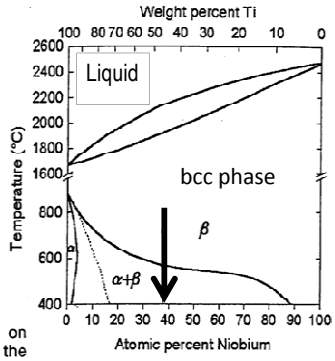

Nb-Ti phase diagram. The low temperature boundaries are based on calculations by Kaufman et al. The dashed line represents the martensitic transformation inferred by Moffatt and Larbalestier.

The fabrication of NbTi wires

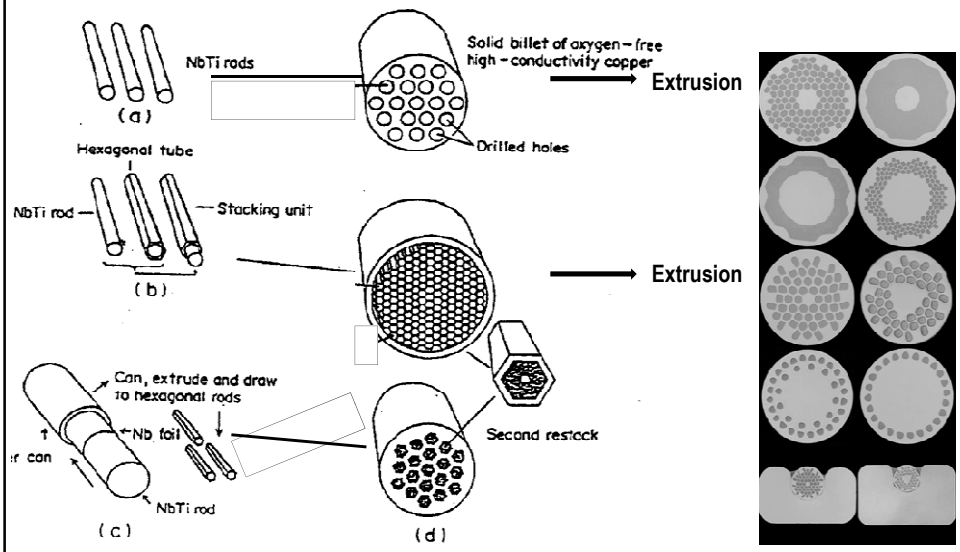

TEM image of NbTi filaments

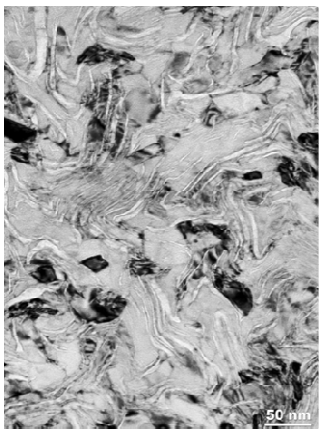

Courtesy Oxford Instruments

α – Ti ribbons: form spontaneously during wire deformation

TEM image of the microstructure (transverse cross-section) of a 3700 A/mm² (5 T, 4.2 K) multifilamentary strand from Oxford Instruments (OST).

This image shows the dense array of folded α-Ti ribbons (lighter contrast) that create the strong vortex pinning.

D. Larbalestier and P. Lee, 1995

Artificial pinning centers in NbTi

Artificial pinning: Introducing defects having sizes comparable or smaller than ξ_o

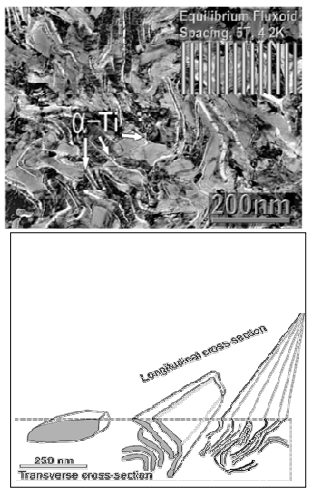

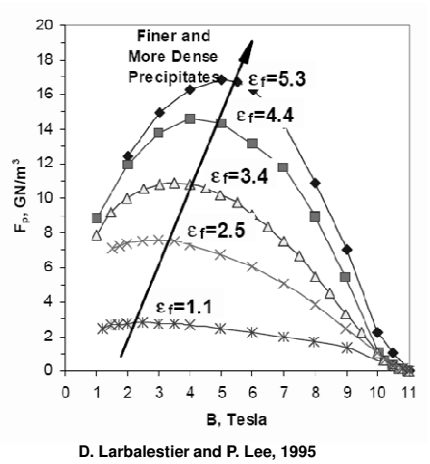

D. Larbalestier and P. Lee, 1995

Artificial pinning

Progress in j_c of Nb-Ti wires with Nb APC (L. Cooley, D. Larbalestier)

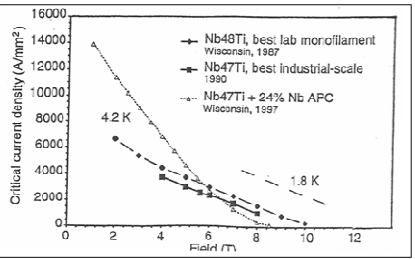

Today, NbTi is used * for NMR up to 9T,
* for a background field in high field magnets
and * for accelerator magnets (LHC)

No further work is performed for a further enhancement of J_c in industrial NbTi wires.
Artificial pinning in Nb_3Sn was so far unsuccessful.

The system Nb_3Sn

V. The system Nb_3Sn

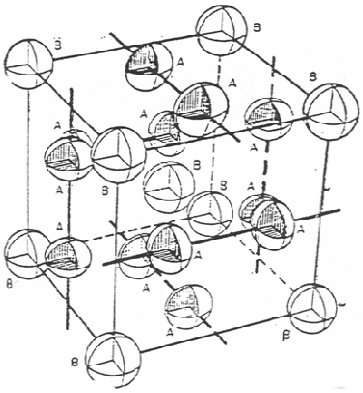

The cubic A15 type structure A_3B

The system Nb_3Sn

Very brittle phase ; $T_c = 18$ K, $B_{c2} = 22$T (clean limit : $l >> \xi_0$)
$B_{c2} = 30$ T (dirty limit : $l \approx \xi_0$)

Perfectly ordered phase : all cubic sites occupied by Sn
all chain sites occupied by Nb

→ very low normal state electrical resistivity $\rho(T>T_c)$, or ρ_c

The Nb-Sn phase diagram

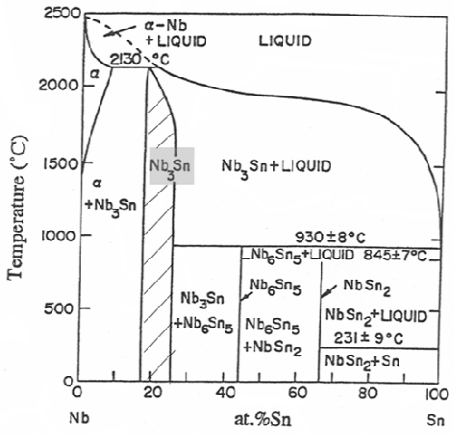

T> 43K: cubique
T< 43K : tetragonal

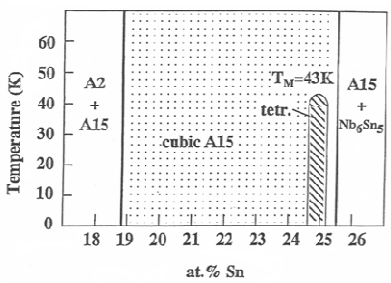

High temperature **Low temperature**

A. Superconducting properties of the A15 phase

Variation of T_c with Sn content in Nb_3Sn

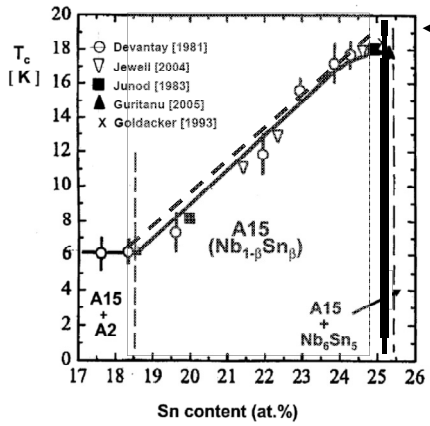

T_c(linear extrapolation): ~ 19 K

Saturation at > 24.5 at.%:

Due to phonon softening

$T_c = T_c$(max) at 25 at.% Sn

$T_c = T_{c\,max} =$ 18.3 K at the stoichiometric composition (25 at.%Sn):

Variation of ρ_o vs. Sn content in Nb_3Sn

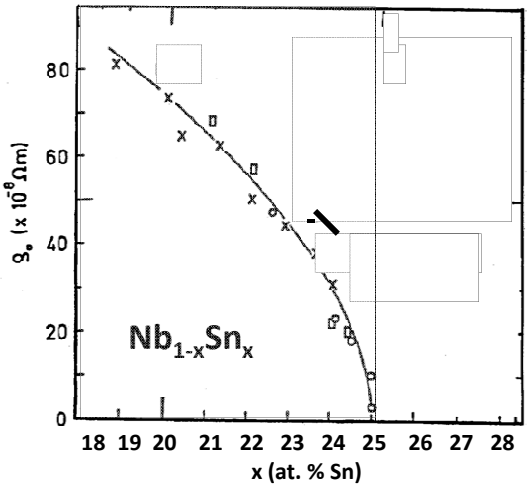

$\rho_o = \rho_o$(min) at 25 at.% Sn:

< 10 μΩcm

Variation of B_{c2} vs. Sn content in Nb_3Sn

$B_{c2} = B_{c2}(max)$

at ~ 24.5 at.% Sn

Not at 25 at.% Sn!

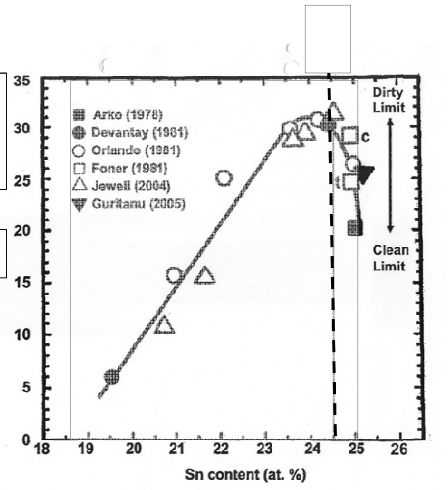

Effect due to electronic mean free path: ρo

$B_{c2} \sim T_c\ \gamma\ \rho_o$

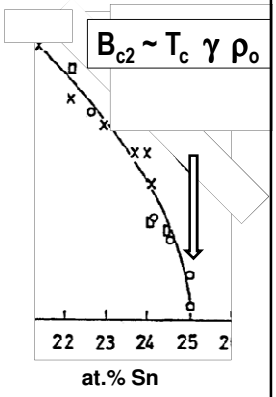

Clean and dirty limit in Nb_3Sn

$B_{c2} \sim T_c\ \gamma\ \rho_o$

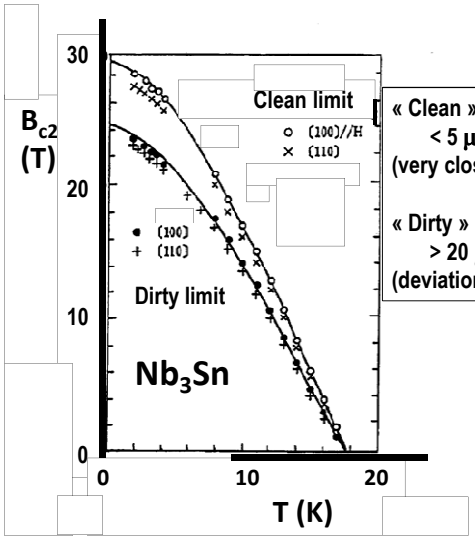

« Clean » limit: low ρ_o
< 5 μΩcm
(very close to stoichiometry)

« Dirty » limit: high ρ_o
> 20 μΩcm
(deviation from stoichiometry)

Enhancement of J_c at high fields by Ta and Ti additives

Effect of Ti and Ta additives

Ta: Cody et al. (1972)
Ti: Sekine et al. (1980)
Drost et al. (1985),
Suenaga et al., (1986),
Geneva group (2007)

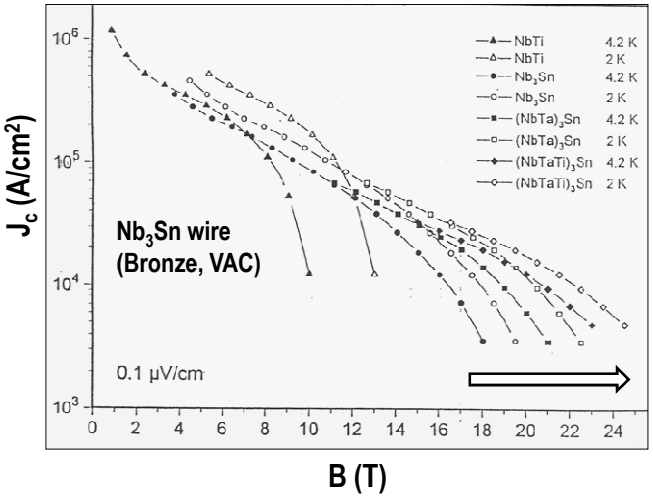

Effect of Ta and Ti alloying on T_c of Nb_3Sn

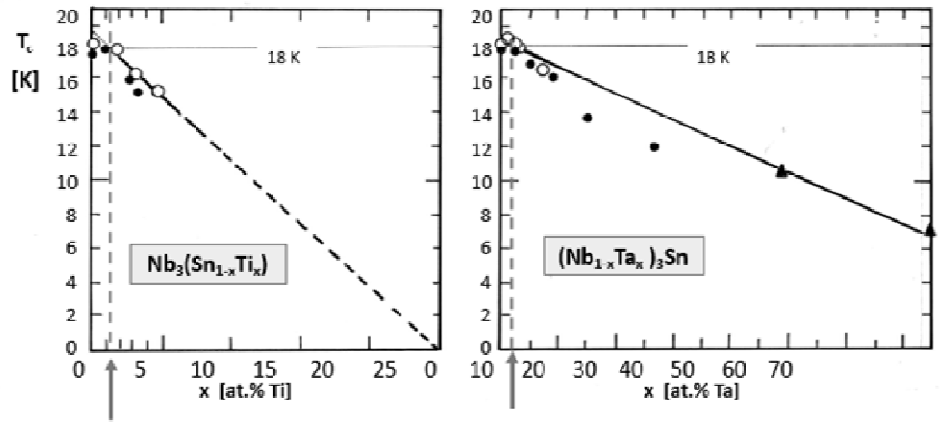

The variation of T_c for the Ta and Ti content giving the highest values of J_c is very small

Enhancement of J_c at high fields by Ta and Ti additives

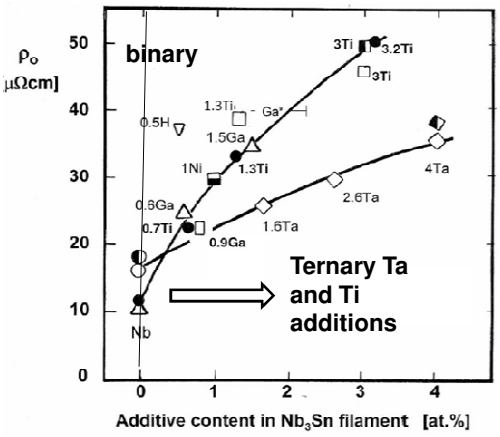

Effect of Ta and Ti additives:

⇒ **Enhancement of ρ_o**

Since $B_{c2} \sim T_c\ \gamma\ \rho_o$, and ΔT_c and $\Delta\rho_o$ small:

$\rho_o \nearrow \Rightarrow B_{c2} \nearrow$

B. Wire fabrication and critical current densities

Nb_3Sn wires

Industrial fabrication techniques

A: Bronze Route
B: Internal Sn Diffusion
C: Powder in Tube (or PIT) method

The diffusion - reaction pattern for Nb_3Sn

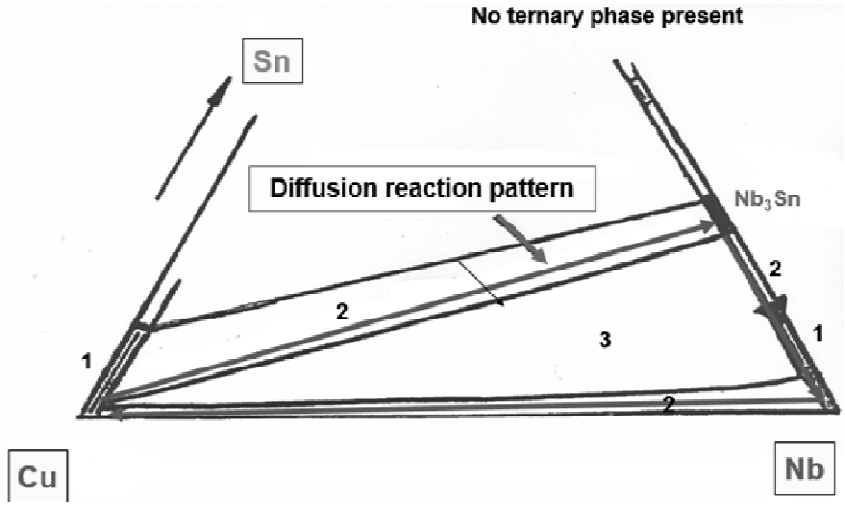

The bronze diffusion reaction to Nb_3Sn

Conditions after reaction

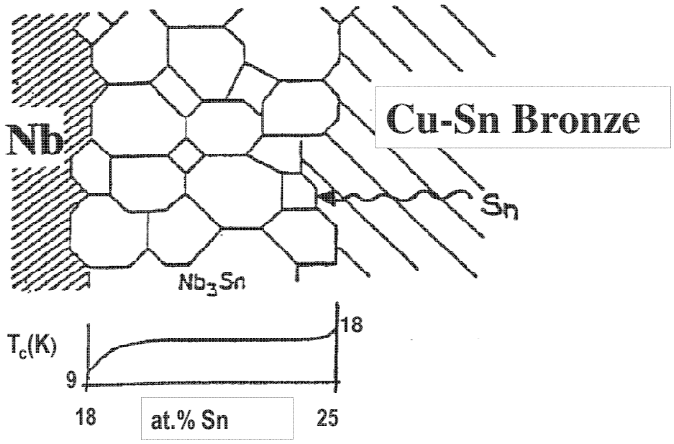

Techniques for the Nb_3Sn wire fabrication

The CERN Accelerator School

Several different industrial modes of processing Nb_3Sn wires.

1: High Sn contents (>18 wt.% Sn)

Internal Sn, Filaments:	IGC (USA), Alsthom (F), Eurometalli (I)
Internal Sn, Jelly Roll:	**Oxford (USA)**
Nb tube process:	Showa, Toshiba (J)
ECN route : powder process	SMI (Ne)

High Sn content leads to higher values of j_c (distribution in the filaments)

2: Low Sn contents (≤ 15.4 wt.%Sn)

Bronze route:	VAC (D), Kobe Steel (J), Hitachi (J), Furukawa (J)

The bronze route is the only one being appropriate to persistent mode operation of a solenoid, since the Ta barrier can be set at the tenter of the wire : the contacts between filaments of two joints occurs directly from superconductor to superconductor (the Ta barrier does not need to be etched away).

Processing of Bronze route and Internal Sn diffusion Nb3Sn wires

The CERN Accelerator School

Bronze Route: With intermediate anneals

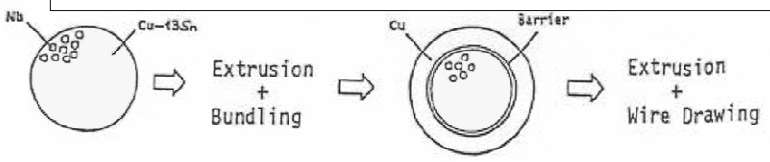

Internal Sn Diffusion method: No intermediate anneals

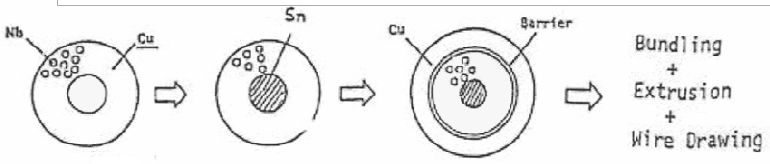

Bronze Route wires, advantages

Bronze route

Minus

- Intermediate anneals each 50 % of cross section reduction
- Lower j_c values than Internal Sn wires at intermediate and low fields

Plus

- Very long lengths (> 5'000 m)
- Low effective filament diameter (< 20 μm)
- High longitudinal homogeneity
- Appreciably high j_c values at high fields
- Suitable for persistent mode applications (central Ta barrier around Cu stabilizer)

* Has the best mechanical properties of all Nb_3Sn wire types

Internal Sn Diffusion wires

Internal Sn route

Minus

- Effective diameter higher than for bronze route
- Longitudinal homogeneity lower than for bronze route
- Less uitable for persistent mode operation (external Ta barrier)

Plus

- No intermediate anneals (lower costs than bronze route wires)
- High j_c values at intermediate fields : > 3'500 A/mm^2 at 4.2K/12T
- Appreciably long lengths (> 1'000 m)

Multifilamentary Nb_3Sn wires

Nb_3Sn: T_c = 18K, $H_{c2}(0)$ = 30T

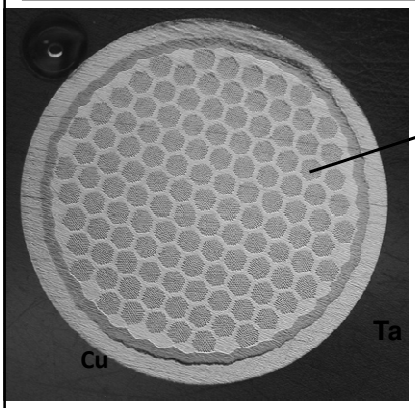

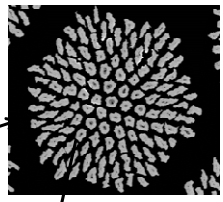

Filament group

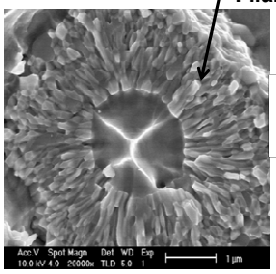

Filament diameter 4 μm)

Grain sizes: 100 – 200 nm

Bronze type Nb_3Sn wire (10'000 filaments)

The Bronze Route

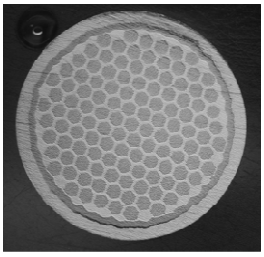

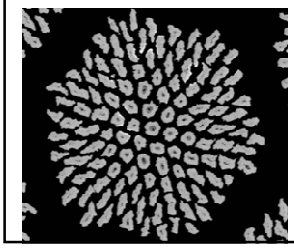

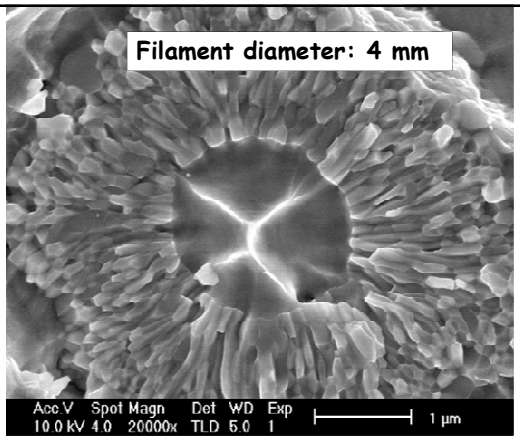

V.Abächerli et al., ASC 2004

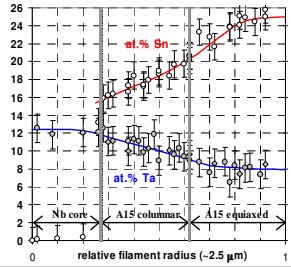

Limitation: only a small part of the filament carries supercurrent !

Summer School_06

Nb_3Sn wire configuration by Internal Sn diffusion

2 RRP wires with J_c (non-Cu) = 2'000 A/mm² at 4.2K/12T

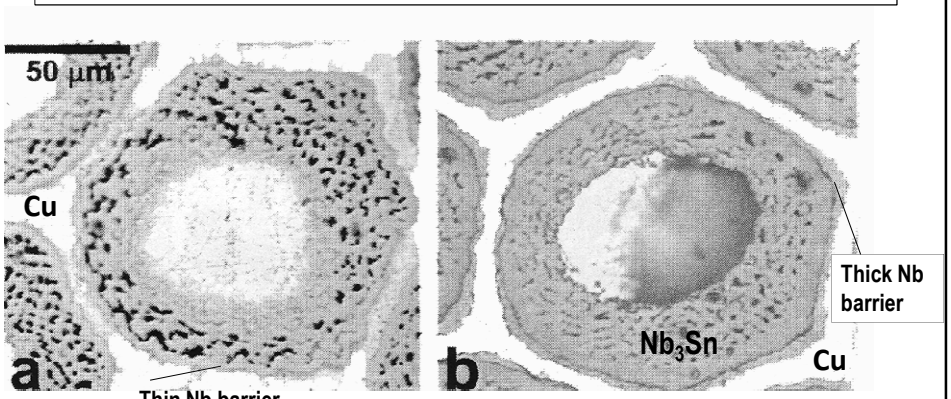

a: thin Nb barrier, almost fully reacted: RRR = 10

b: thick Nb barrier, a complete unreacted Nb barrier remains: RRR = 100.

NbTi addition in Internal Sn wires (OST)

Ti additives introduced by NbTi rods.

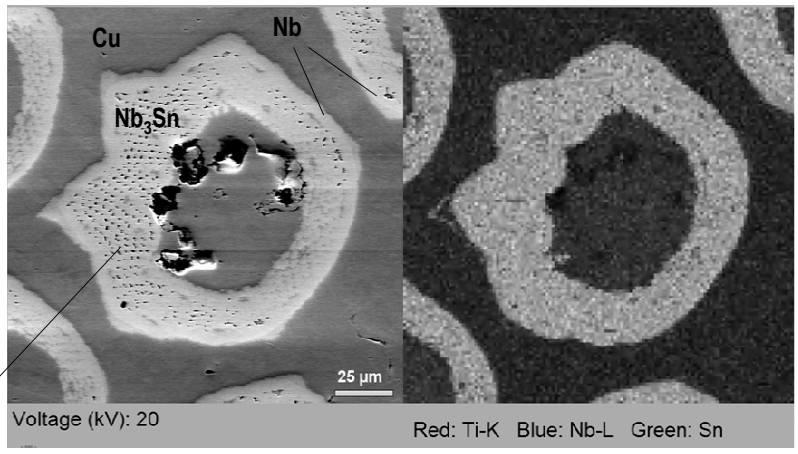

Ti (from NbTi)

P. Lee, D. Larbalestier, J.A. Parrell, M.B. Field, Y. Zhang, S. Hong, ICMC 05, Keystone, USA

Optimized Nb_3Sn reaction

Required for LHC Upgrade: J_c(non-Cu) = 1'500 A/mm² at 4.2K/15T

1mm Ti doped 169 stack strand (D_s~52µm)

Study of heat treatment temperature 665ºC and 650ºC

- trade small decrease of 15 T J_c to improve RRR > 200

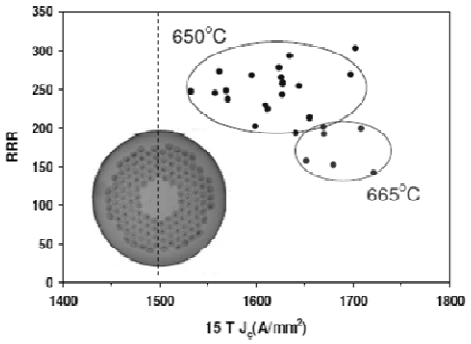

Courtesy Parrell (OST)

RRP wires for various applications

Distributed Barrier Internal Sn – RRP®

- Conductor development focused on the needs of the application
  - NMR – highest J_c at high field, D_{eff} generally not a concern
  - HEP – high J_c at mid field, but with small D_{eff}
  - CICC – mid J_c at mid field, with high RRR after Cr plating
  - Lab magnets – a large I_c range (wire diameter selection), strength

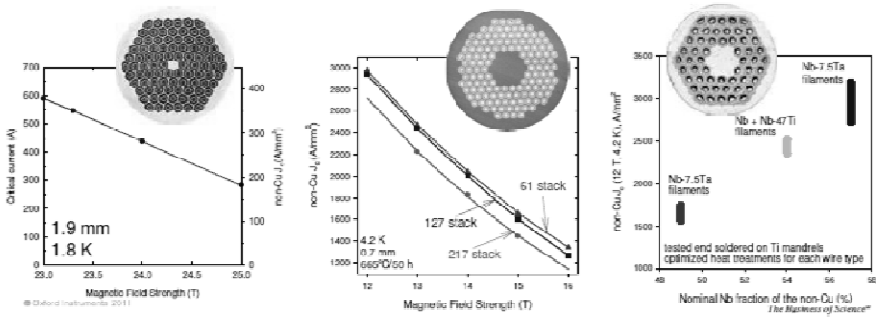

Courtesy Parrell (OST)

Powder in Tube (or PIT) technique

PIT technique

Minus
- Mechanical properties
- Large effective filament diameter
- * Higher costs than other techniques

Plus
- Very high Sn content → constant Sn level in the filaments
- Very high cirtical current densities > 3'000 A/mm^2 at 4.2K/12T

As starting material, one uses $NbSn_2$ powders, which are difficult to fabricate
⇨ high costs

PIT: Powder in tube Nb_3Sn wires

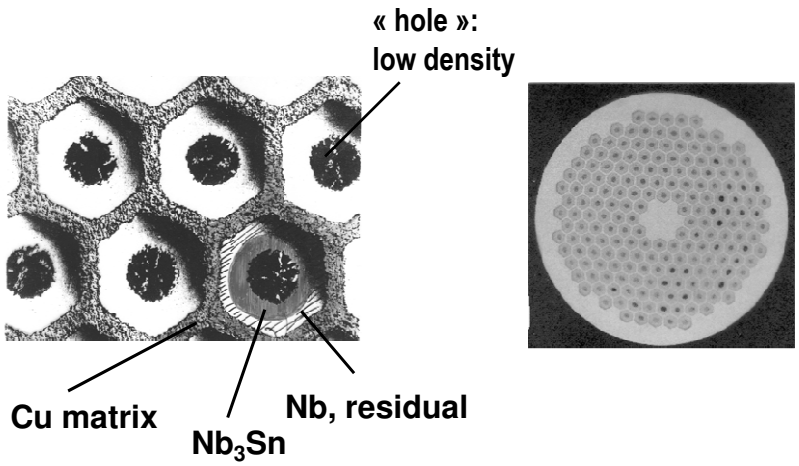

C. Calorimetric analysis of Nb_3Sn wires

Specific heat measurements:

- No shielding effects
- Measures the totality of the superconducting volume in the wire
- Measurement with the matrix (under prestress)
- Up to high fields (21 T)

Technique

- Measurement at 0T and 14T
- Subtraction, to eliminate normal conducting part
- Deconvolution of the superconducting part ⇨ T_c distribution

Result: All Nb_3Sn wires are inherently inhomogeneous! Susceptibility or resistivity measurements give only the onset value of T_c!

T_c distribution from specific heat measurements

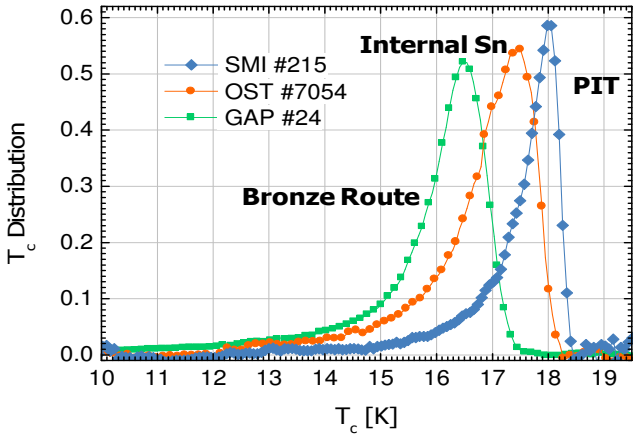

Clear difference between Bronze route and Internal Sn (RRP) wires:
Bronze Route wires have a lower T_c ⇨ lower average Sn content

C. Senatore, V. Abächerli, R.Flükiger, 2011